

# RNA polymerase III drives alternative splicing of the potassium channel–interacting protein contributing to brain complexity and neurodegeneration

Sara Massone,<sup>1</sup> Irene Vassallo,<sup>1</sup> Manuele Castelnovo,<sup>1</sup> Gloria Fiorino,<sup>4</sup> Elena Gatta,<sup>2</sup> Mauro Robello,<sup>2</sup> Roberta Borghi,<sup>3</sup> Massimo Tabaton,<sup>3</sup> Claudio Russo,<sup>5</sup> Giorgio Dieci,<sup>4</sup> Ranieri Cancedda,<sup>1</sup> and Aldo Pagano<sup>1</sup>

<sup>1</sup>Department of Oncology, Biology, and Genetics, National Institute for Cancer Research, <sup>2</sup>Department of Physics, and <sup>3</sup>Department of Experimental Medicine, University of Genoa, I-16132 Genoa, Italy

<sup>4</sup>Department of Biochemistry and Molecular Biology, University of Parma, 43121 Parma, Italy

<sup>5</sup>Department of Health Sciences, University of Molise, Campobasso, 86100 Molise, Italy

**A**lternative splicing generates protein isoforms that are conditionally or differentially expressed in specific tissues. The discovery of factors that control alternative splicing might clarify the molecular basis of biological and pathological processes. We found that IL1- $\alpha$ –dependent up-regulation of 38A, a small ribonucleic acid (RNA) polymerase III–transcribed RNA, drives the synthesis of an alternatively spliced form of the potassium channel–interacting protein (KCNIP4). The alternative KCNIP4 isoform cannot interact with the  $\gamma$ -secretase complex, resulting in modification of  $\gamma$ -secretase activity,

amyloid precursor protein processing, and increased secretion of  $\beta$ -amyloid enriched in the more toxic A $\beta$  x-42 species. Notably, synthesis of the variant KCNIP4 isoform is also detrimental to brain physiology, as it results in the concomitant blockade of the fast kinetics of potassium channels. This alternative splicing shift is observed at high frequency in tissue samples from Alzheimer's disease patients, suggesting that RNA polymerase III cogenes may be upstream determinants of alternative splicing that significantly contribute to homeostasis and pathogenesis in the brain.

## Introduction

The potassium channel–interacting protein (KCNIP4, also known as KChIP4; NCBI Protein database accession no. NP\_079497.2) is a physical interactor of the  $\alpha$  subunit of Kv4, a neuronal A-type voltage-dependent potassium channel (Kitagawa et al., 2007). By the means of such an interaction, it participates in the regulation of the A-type current needed for the generation of slow repetitive firing in neurons, thus strongly contributing to the molecular properties of potassium channels (Etcheberrigaray et al., 1993; Shibata et al., 2003; Rhodes et al., 2004). Previous work demonstrated that KCNIP4 also interacts *in vivo* and in HEK293 cells with presenilins (PSs), the key components of the  $\gamma$ -secretase complex that processes the amyloid precursor protein (APP) to generate the A $\beta$  fragments involved in Alzheimer's disease (AD; Morohashi et al., 2002; Parks and

Curtis, 2007). A set of possible KCNIP4 alternative splicing variants with peculiar biochemical and biophysical properties may account for a complex pattern of splice form–dependent protein–protein interactions (Deng et al., 2005; Pruunsild and Timmusk, 2005). In this context, the canonical splice variant 1 (also referred to as KChIP41b and hereafter referred to as Var I) is widely expressed in all of the brain cell components tested, whereas the alternatively spliced KCNIP4 variant 4 (also referred to as KChIP4a and hereafter referred to as Var IV; Fig. S1, A and B) is specifically expressed in the globus pallidus and basal forebrain neurons (Baranauskas, 2004; Trimmer and Rhodes, 2004). Notably, these alternatively spliced cell type–specific KCNIP4 variants also account for changes of the A-type current among different cell types (Patel et al., 2002; Boland et al., 2003; Decher et al., 2004). In fact, the fast inactivation of the A-type current physiologically associated with Kv4 channels, which takes place when KCNIP4 is canonically spliced to Var I, is rapidly

S. Massone, I. Vassallo, and M. Castelnovo contributed equally to this paper.

Correspondence to Aldo Pagano: aldo.pagano@unige.it

Abbreviations used in this paper: AD, Alzheimer's disease; APP, amyloid precursor protein; ChIP, chromatin immunoprecipitation; DREAM, downstream regulatory element antagonist modulator; GAPDH, glyceraldehyde 3 phosphate dehydrogenase; LTP, long-term potentiation; nA $\beta$ c, non-AD control; ncRNA, noncoding RNA; PEI, polyethylenimine; PS, presenilin; PSE, proximal sequence element; rRNA, ribosomal RNA; wt, wild type.

© 2011 Massone et al. This article is distributed under the terms of an Attribution–Noncommercial–Share Alike–No Mirror Sites license for the first six months after the publication date [see <http://www.rupress.org/terms>]. After six months it is available under a Creative Commons License (Attribution–Noncommercial–Share Alike 3.0 Unported license, as described at <http://creativecommons.org/licenses/by-nc-sa/3.0/>).

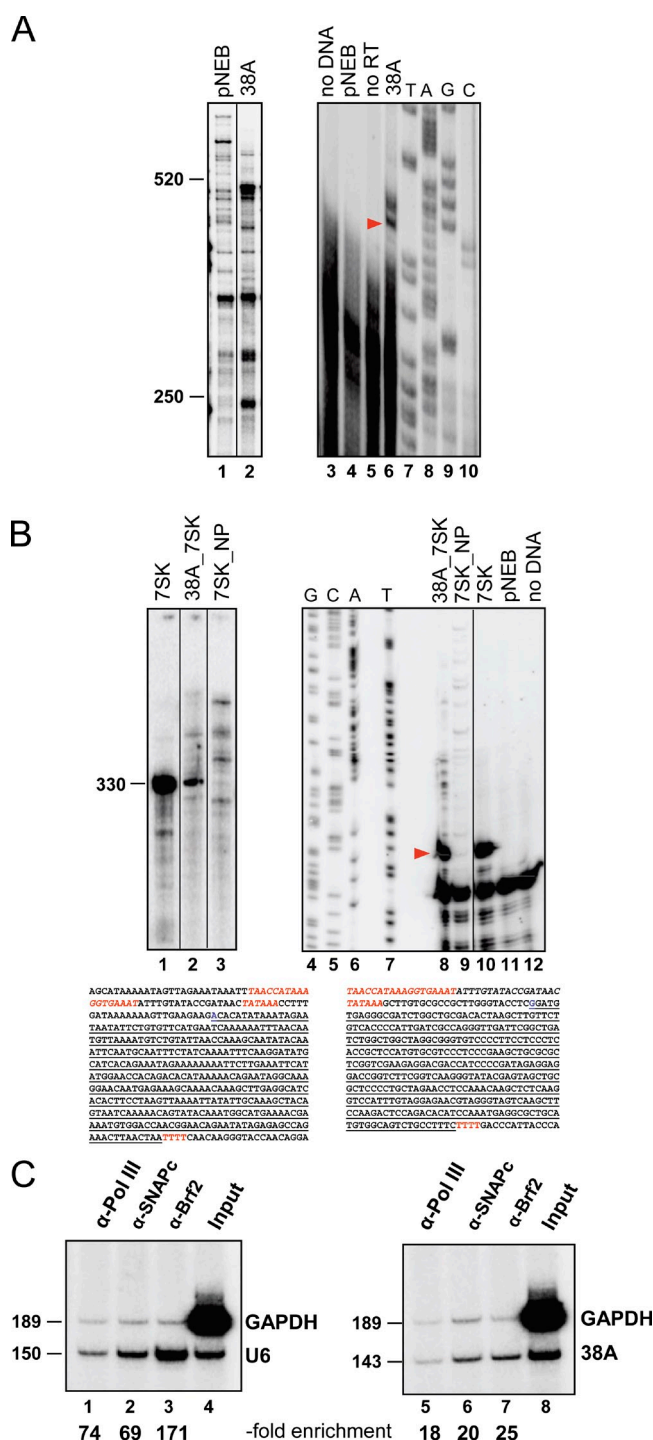


**Figure 1. In vitro transcription analysis of 38A.** (A) Transcription products of 38A or empty vector (pNEB) were either radiolabeled during synthesis and directly visualized (lanes 1 and 2) or subjected to primer extension analysis (lanes 3–6; lane 3, no DNA; lane 5, no reverse transcription). In lane 6, the main primer extension product is indicated by a red arrowhead. Lanes 7–10 are sequencing reactions primed with the same oligonucleotide. The sequence of the 38A transcription unit is reported (PSE, TATA, and terminator in red, transcription start site in blue, and transcribed region underlined). (B) In vitro transcription and primer extension analysis with the human 7SK gene (lanes 1 and 10), promoterless 7SK (lanes 3 and 9), and the 7SK transcribed region fused with 38A promoter (lanes 2 and 8) as templates. The sequence of the hybrid transcription unit is reported (PSE, TATA, and terminator sequences in red and the 38A-derived upstream sequence in italic). The red arrowhead indicates the position of the most abundant primer extension product. (C) ChIP analysis in SHSY5Y-cultured cells using

transformed in a slowly inactivated potassium current when an alternative splicing event leads to the synthesis of KCNIP4 Var IV as a result of reduced trafficking of Kv4 channels to the surface membrane (Holmqvist et al., 2002; Schwenk et al., 2008). This condition is associated with an impairment of the electrophysiological properties of the cell, affecting the excitatory or the inhibitory back-propagating action potentials that ultimately participate in associative events such as long-term potentiation (LTP) and long-term depression. In addition, possible cis- or trans-acting factors that select the alternative splicing forms could drive the cell to an altered synaptic behavior based on the impairment of its excitatory properties. Moreover, the notion that a perturbation of LTP might contribute to the phenotypic manifestations of neurodegeneration, together with the fact that the other KCNIP4 partners (the PSs) are deeply involved in the etiology of AD, strongly suggests a possible involvement of KCNIP4 alternative splicing in neurodegenerations.

This work originates from our recent identification of a set of 30 RNA polymerase III (PolIII)–dependent noncoding RNAs (ncRNAs) that we proposed as novel gene expression regulatory elements acting by the generation of specific PolIII/PolII cogene/gene pairs (Dieci et al., 2007; Pagano et al., 2007). Interestingly, one of these transcripts (hereafter referred to as 38A) maps within KCNIP4 gene intron 1, a region involved in the alternative splicing events leading to Var IV of KCNIP4 (Fig. S1, A and B). Considering the antisense configuration of 38A with respect to KCNIP4 intron 1, we hypothesized that KCNIP4 pre-mRNA and 38A ncRNA might form a sense/antisense RNA pair, thus masking KCNIP4 canonical splice sites and leading to the synthesis of alternatively spliced forms possibly associated with peculiar pathological conditions. Here, we report evidence that 38A is indeed the first player of a novel molecular pathway that leads to the altered amyloid production associated with AD etiology as well as with the perturbation of the A-type current that ultimately leads to the impairment of cellular excitatory properties. We further report that inflammatory stimuli trigger 38A-dependent alternative splicing, thus providing a molecular link between inflammation and the etiology of neurodegeneration, and we describe some allelic variants of the 38A promoter that might contribute to enhancing the genetic susceptibility of certain individuals to the activation of this pathological process.

## Results

### 38A ncRNA is transcribed by RNA PolIII

The putative 38A ncRNA gene was identified in a previous computational screen for novel human PolIII target genes (Pagano et al., 2007). First, we verified 38A activity as a PolIII template

anti-PolIII, anti-SNAPc, or anti-Brf2 antibodies. Association with the GAPDH control gene and either the U6 gene (lanes 1–4) or the 38A locus (lanes 5–8) was assessed by PCR on both input (lanes 4 and 8) and immunoprecipitated DNA samples interrogated with both target-specific and control primer pairs. Target enrichment in the immunoprecipitated DNA is reported below the lanes. (A and B) Black lines indicate that intervening lanes have been spliced out. Molecular mass is indicated in base pairs..

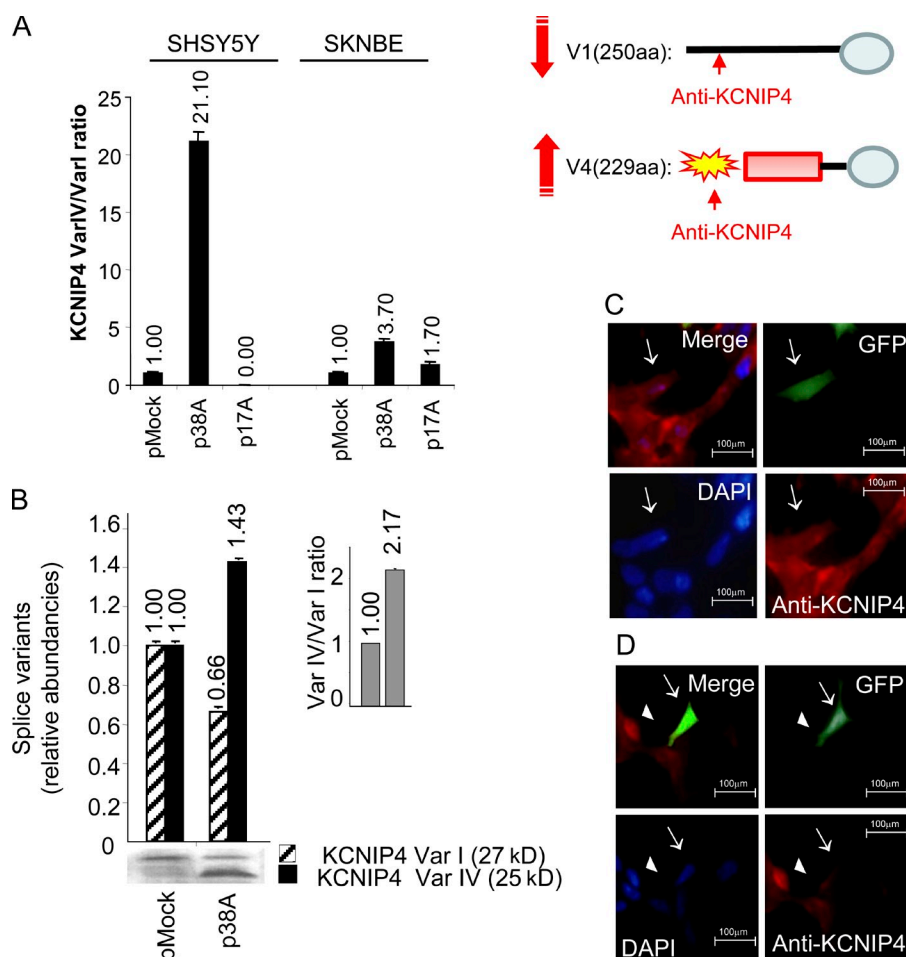


**Figure 2. ncRNA-induced alternative splicing analysis.** (A) Real-time RT-PCR detection of KCNIP4 splice variant synthesis in SHSY5Y and/or in SKNBE cells transiently transfected with either 38A or 17A (a noncorrelated PolIII-transcribed ncRNA used as a negative control) expression plasmids. Altogether, these results indicate that each ncRNA specifically influences the splicing of its corresponding protein-coding gene. (B) Western blotting analysis of the 38A-dependent alternative splicing of KCNIP4. In pMock-transfected cells, the relative abundance of the 250-residue-long form of KCNIP4 (Var I, striped bars) is predominant with respect to the alternatively spliced 229-residue-long form (Var IV, shaded bars) that, in turn, is the main KCNIP4 form synthesized by p38A-transfected cells. Quantitative bars and the correspondent error bars (SD) are referred to the mean of three independent experimental determinations (A and B). The p38A-dependent change of Var IV versus Var I protein form ratio is quantitatively reported (inset in B). (C and D) Immunofluorescence detection of KCNIP4 alternative splicing. Antibodies raised against the KCNIP4 N-terminal fragment of the protein form I show a clearly detectable signal in GFP-expressing cells only in the absence of a concomitant 38A overexpression (arrows in C); on the contrary, the signal is absent or very weak in cells transfected with a construct coexpressing 38A and GFP (arrows in D). Untransfected cells, which do not express GFP and 38A, are positive for KCNIP4 (arrowheads in D).

in vitro using a HeLa cell nuclear extract. As shown in Fig. 1 A, in vitro transcription of a plasmid-borne 38A construct containing the upstream proximal sequence element (PSE) and the TATA box, followed by the putative 352-bp transcribed region, produced RNAs of different sizes (lane 2); primer extension analysis (lanes 3–10) revealed that transcription initiated ~30 bp downstream of the TATA box. As further shown in Fig. 1 B, the 38A promoter region was also found to be active in directing faithful 7SK gene transcription in fusion constructs. The association of the 38A transcription unit with PolIII-specific transcription proteins was tested in vivo by chromatin immunoprecipitation (ChIP) analysis. Fig. 1 C shows the results of a ChIP analysis conducted on SHSY5Y-cultured cells using anti-Brf2 (a TFIIB component), anti-SNAP43 (a SNAP-C component), and anti-RPC39 (a PolIII subunit) antibodies. 38A was found to be specifically enriched in all the immunoprecipitations.

### 38A transcription drives KCNIP4 alternative splicing

We then tested whether the overexpression of 38A causes a gene-specific alternative splicing shift of KCNIP4. To this end, we focused on the two physiologically relevant splice variants Var I and Var IV. We transiently transfected SHSY5Y and SKNBE neuroblastoma cells (Biedler et al., 1973; Biedler and Spengler, 1976) with a construct expressing 38A transcript (driven by its

natural promoter) and measured changes in the levels of Var I and Var IV mRNAs by real-time RT-PCR. As shown in Fig. 2 A, 48 h after transfection, a remarkable alteration of Var IV versus Var I ratio was detected (21.1 vs. 1) in SHSY5Y cells as a consequence of an increased generation of Var IV and a decreased synthesis of Var I. The same result was obtained with SKNBE cells, although this cell type transcribes 38A less efficiently. Overexpression of 17A, a distinct PolIII-transcribed regulatory RNA that maps in an unrelated locus, did not exert any effect on KCNIP4 pre-mRNA maturation. Altogether, these results indicate that 38A overexpression is sufficient to drive the alternative splicing shift of KCNIP4 mRNAs, promoting the synthesis of the Var IV isoform. With respect to Var I, this isoform encompasses a KIS domain in its N terminus that enables it to inhibit the fast kinetics of inactivation of A-type voltage-dependent potassium channels (Holmqvist et al., 2002).

The 38A-driven alternative splicing was also evidenced at the protein level. Taking advantage of a KCNIP4-specific antiserum raised against an internal region of the human protein (hereafter referred to as KChIP4-L14), we detected a significant increase of KCNIP4 signal at ~25 kD and a concomitant decrease of the signal at 28 kD. The relative abundance of the two KCNIP4 forms was quantified as a Var IV versus Var I protein ratio, and it was increased ~2.2-fold in p38A-transfected cells as compared with those transfected with pMock (Fig. 2 B).



To verify the PolIII dependency of this phenomenon, we prevented the expression of 38A by a treatment with 20  $\mu$ M ML-60218, an RNA PolIII-specific inhibitor (Fig. S2; Wu et al., 2003).

Alternative splicing control by 38A is further supported by the results of immunofluorescence microscopy analysis. Using a polyclonal antibody raised against the N terminus of KCNIP4 Var I (KChIP4 N-14), we observed a marked immunofluorescence signal in pMock-transfected SHSY5Y cells; in this condition, 38A is not overexpressed, and the canonical Var I is predominantly synthesized (Fig. 2 C). In contrast, a strongly decreased signal was detected in cells overexpressing 38A where the alternative protein form IV (harboring a different N-terminal portion and not recognized by the same IgGs) is predominant, whereas the synthesis of KCNIP4 Var I was strongly decreased (Fig. 2 D). Altogether, the aforementioned results support the model of 38A as a key supervisor of the synthesis of functionally different KCNIP4 protein isoforms and bring to light a novel, unexpected role of PolIII-transcribed ncRNAs in gene expression regulation.

### 38A expression prevents the fast inactivation of A-type K<sup>+</sup> channels

KCNIP4 Var IV is known to influence the cell excitatory properties by abolishing the fast inactivation of A-type potassium channels on which rapid neuron firing depends (Baranauskas, 2004). Such alteration has been associated with neurodegenerative processes (Angulo et al., 2004; Waters et al., 2006). To test whether 38A expression can perturb the excitatory properties of synapses in neurons, we first searched for the proper cell culture system for the determination of the A-type current. SKNBE-NDM29 cells (a SKNBE clone with characteristics of neurons; Castelnuevo et al., 2010) turned out to be a system in which this current is well detected. We transfected these cells with plasmids harboring 38A under the control of its natural promoter (pEGFP-N1-38A) and/or without insert (pEGFP-N1). 48 h after transfection, we measured the inactivation time in a large panel of cells for each sample. Fig. 3 shows the outward potassium current elicited in control (Fig. 3 A) and in 38A cells (Fig. 3 B) by depolarization steps from a  $-80$ -mV holding potential. The inactivation time course of this current could be described by a single exponential curve. In 75% of 38A cells, the time constant of the inactivating potassium current was increased. The time constant of the current elicited by depolarizing steps to 60 mV was found to be close to 1,130 ms in the 38A cells as opposed to the time constant (580 ms) of the control cell current. Considering the transfection efficiency (70–80%), virtually all of the 38A-expressing cells are affected. When the same cells were transfected with constructs expressing the alternatively spliced KCNIP4 Var IV and/or the N-terminal KIS domain specifically coded by Var IV, both conditions produced the inactivation of potassium current, recapitulating the same effect elicited by 38A overexpression (Fig. 3, C–F). Altogether, these data demonstrate that 38A can abolish the fast inactivation of the A-type voltage-dependent potassium channels, thus affecting the transient component of their A-type current. Considering that this phenomenon significantly affects the excitatory potentiality of the cell, we concluded that

the activation of 38A expression could be associated with an altered function/state of synapses, as it may occur in neurological disorders.

### 38A-driven alternative splicing abolishes KCNIP4–PS2 interaction

Because it has been previously reported that KCNIP4 interacts with PS2 (NCBI Protein accession no. P49810; Herreman et al., 2000; Morohashi et al., 2002; Bentahir et al., 2006), we tested the two alternative KCNIP4 protein forms for their possible interaction with PS2. 48 h after transfection of SHSY5Y cells with p38A or pMock constructs, we immunoprecipitated KCNIP4 by the KChIP4 L-14 IgGs and analyzed the immunoprecipitation products by SDS-PAGE coupled with Western blotting challenged by the anti-PS2 antibody (PS2 H-76). In pMock-transfected cells, PS2 coimmunoprecipitates with KCNIP4, confirming the previously reported physical interaction (Morohashi et al., 2002). Interestingly, the PS2 signal was significantly decreased in p38A-transfected cells, where KCNIP4 Var IV is predominantly synthesized and recognized by the same antiserum; as the control, another component of the  $\gamma$ -secretase complex (PS1) is not coimmunoprecipitated with KCNIP4 (Fig. 4 A).

When the experiment was repeated in the presence of the PolIII-specific inhibitor ML-60218, PS2 was found to coimmunoprecipitate with KCNIP4 in both pMock-transfected and p38A-transfected cells (Fig. 4 B). The rescue of KCNIP4–PS2 protein–protein interaction by PolIII inhibition and the lack of coimmunoprecipitation of KCNIP4 with another member of the  $\gamma$ -secretase complex (PS1), together with the observation that 38A expression does not affect the level of synthesis of PS2 and/or PS1 (Fig. 4 C), further demonstrates that the PolIII-dependent synthesis of 38A specifically prevents KCNIP4–PS2 protein–protein interaction. Furthermore, it suggests that this phenomenon might affect the role played by PS2 in the  $\gamma$ -secretase complex and, possibly, in APP proteolytic processing. We next tried to corroborate this finding by the immunofluorescence analysis of KCNIP4 Var IV subcellular localization. To this aim, we raised a Var IV-specific antiserum (hereafter referred to as  $\alpha$ -KCNIP4 Var IV) that recognizes a Var IV-specific N-terminal portion (KLLEQFGLIEAGLEC). This antiserum produced a strong protein signal in p38A-transfected cells and a very weak signal in cells permanently transfected with the pMock construct, confirming its specific recognition of the alternative KCNIP4 Var IV (Fig. 4, D and D'). We next took advantage of the  $\alpha$ -KCNIP4 Var I antibody to evidence the colocalization of KCNIP4 Var I and PS2 in SHSY5Y-pMock cells and the lack of it in SHSY5Y 38A-overexpressing cells, coinciding with the data obtained by coimmunoprecipitation (Fig. 4, E and E'). The same analysis was finally repeated using the  $\alpha$ -KCNIP4 Var IV antiserum, showing again that this isoform does not colocalize with PS2 (Fig. 4, F and F'). Altogether, the aforementioned results indicate that the synthesis of KCNIP4 Var IV promoted by 38A expression prevents its physical interaction with PS2, suggesting a possible functional relevance of this alternative splicing shift.

Besides the marked effects driven by the synthesis of KCNIP4 Var IV, it was previously found by others that KChIP3

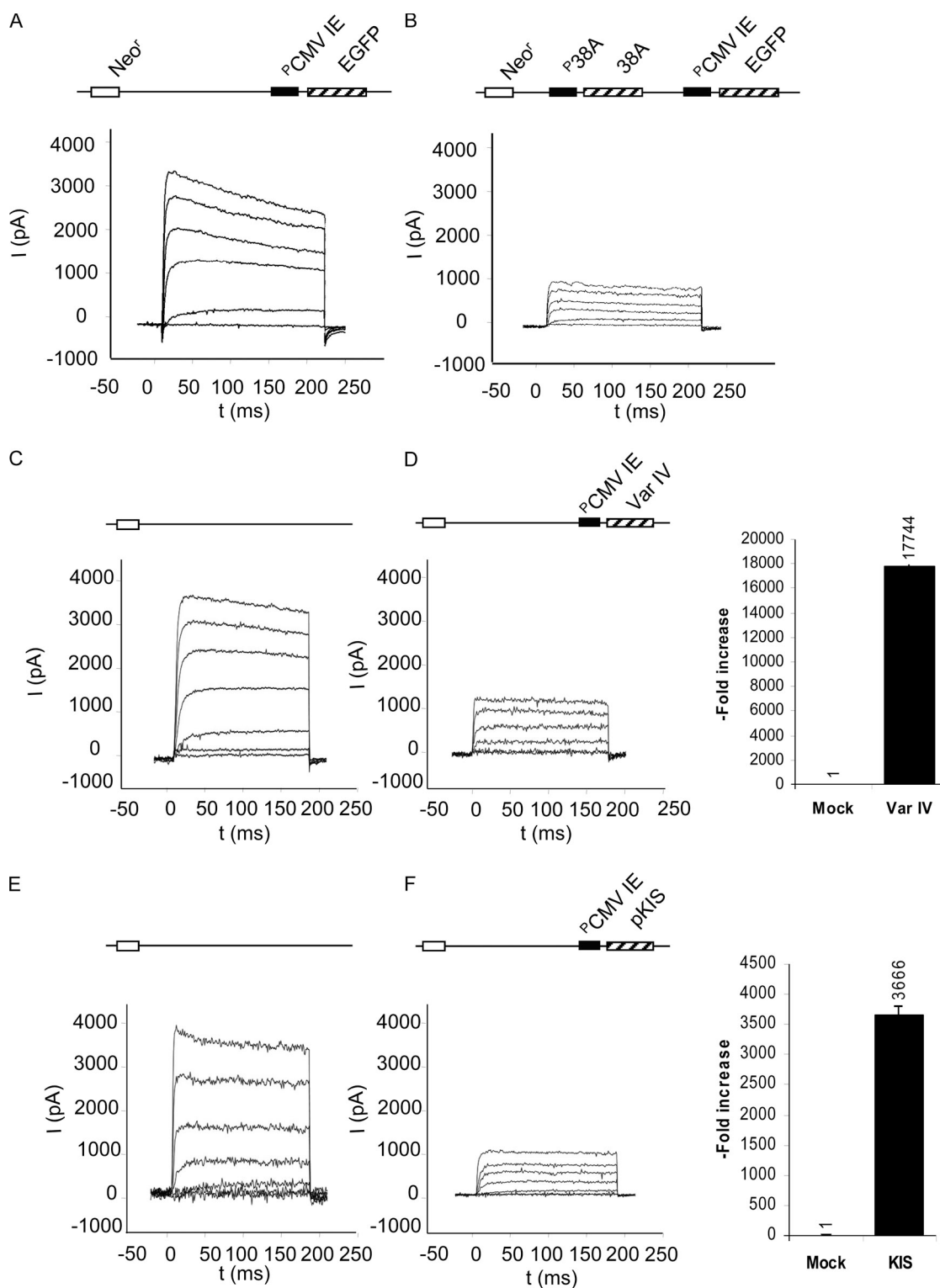


**Figure 3. Effects of 38A expression on A-type potassium current.** (A–F) Outward potassium current in pMock-transfected control cells (A, C, and E), in 38A-overexpressing cells (B), in pETmKChIP4a (D), and in pMaImKIS-transfected cells (F). Step depolarizations were delivered with 20-mV increments. The holding potential was  $-80$  mV. The transient overexpression of the recombinant KCNIP4 Var IV is reported in D as resulting from real-time RT-PCR analysis. The overexpression of the recombinant N-terminal (KIS) domain is reported in F, as resulting from real-time RT-PCR analysis. Error bars are SD.

isoform (namely Calsenilin) also plays a fundamental role in the  $\gamma$ -secretase protein complex-dependent cleavage of the A $\beta$  precursor (Buxbaum et al., 1998). Indeed, KChIP3 is a physical interactor of PS1 and participates in the regulation of the electrical

properties of KV4 channels. We thus tested whether the stable overexpression of 38A in SHSY5Y cells and the consequent synthesis of KCNIP4 Var IV perturb the interaction of Calsenilin with PS1. To this aim, we measured by Western blotting possible

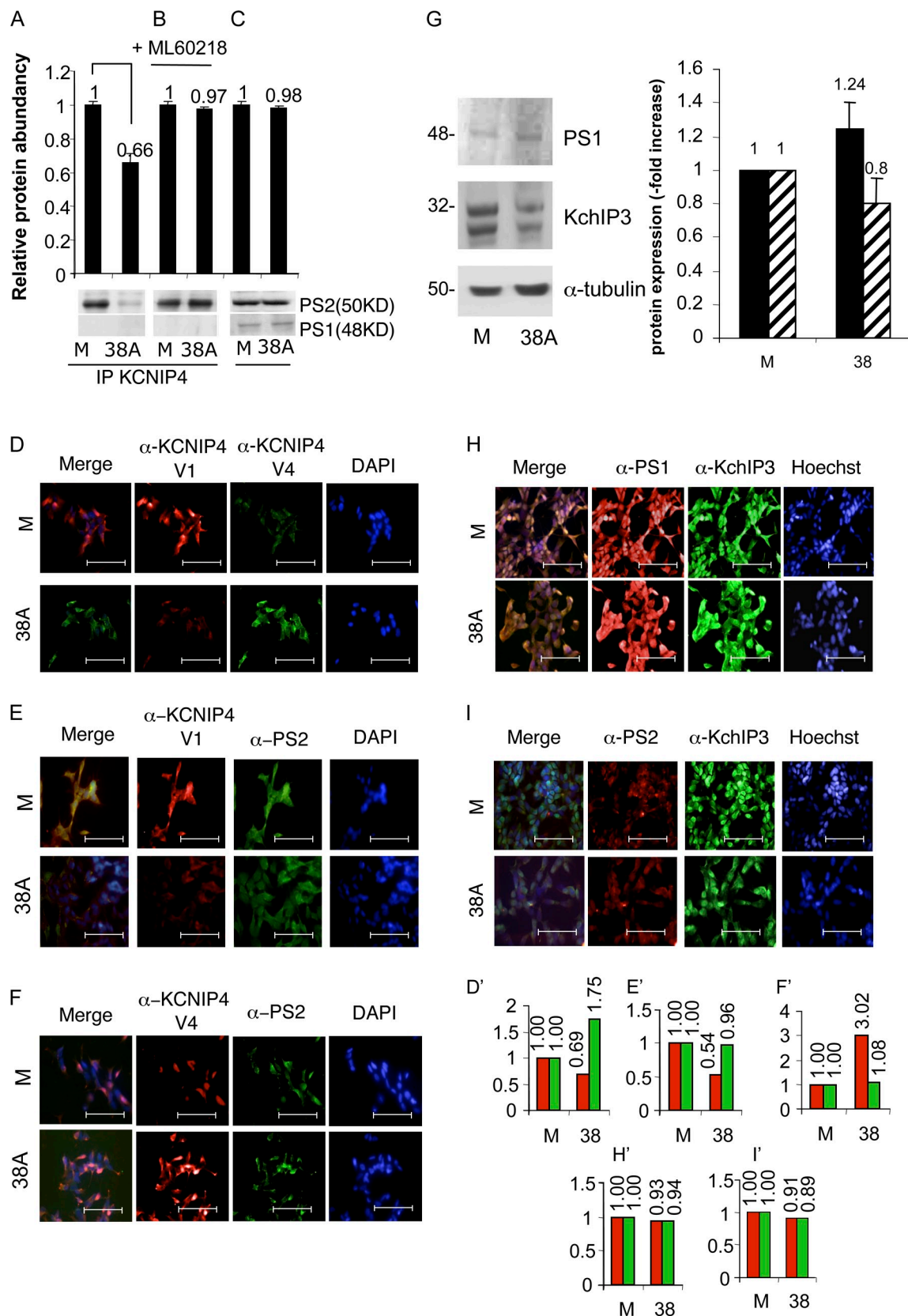


Figure 4. **Lack of KCNIP4–PS2 protein–protein interaction in 38A-overexpressing cells.** (A) PS2 is detected by anti-PS2 IgGs in samples immunoprecipitated (IP) with anti-KCNIP4 in pMock-transfected cells, whereas PS2–KCNIP4 coimmunoprecipitation is prevented in 38A-overexpressing cells ( $P = 0.023$ , as the averaged result of five experiments). In the same samples, the lack of immunoprecipitation of KCNIP4 with a different component of the  $\gamma$ -secretase complex (PS1) is shown. (B) The 38A-dependent impairment of PS2/KCNIP4 protein–protein interaction is prevented by the treatment of cells with the PolIII inhibitor ML-60218. (C) Input sample demonstrating that the amount of PS2 and PS1 in the protein sample is not affected by 38A overexpression.

alterations of PS1 and/or KChIP3 in 38A-overexpressing cells. The statistical analysis of the results showed that the increased expression of 38A does not significantly alter the amount of this protein in the cell (unpaired Student's *t* test: KChIP3 variation, *P* = 0.08; Fig. 4 G). Next, we investigated by immunofluorescence possible changes of the subcellular localization of KChIP3 and/or PSs in 38A-overexpressing cells. Results showed a distinguishable overlapping of  $\alpha$ -anti-PS1 ( $\alpha$ -PS1) and  $\alpha$ -anti-KChIP3 ( $\alpha$ -KChIP3) both in pMock-treated and 38A-overexpressing cells, confirming that KChIP3 colocalizes with PS1 and that their interaction is not affected by the synthesis of KCNIP4 Var IV (Fig. 4, H and H'). Taking advantage of a PS2-specific antiserum, we also found that the overexpression of 38A does not affect the subcellular localization of PS2 (Fig. 4, I and I'). Therefore, our data do not support possible changes of KChIP3 interaction with PSs driven by the increased expression of 38A.

### The expression of 38A specifically enhances the secretion of the neurotoxic A $\beta$ x-42 species

In light of the findings in the previous section and considering that the proteolytic processing of APP plays a central role in AD etiology through the formation of neurotoxic A $\beta$  peptides (Johnson et al., 1990; Selkoe, 1990; Hardy and Selkoe, 2002; St George-Hyslop and Petit, 2005; Haass and Selkoe, 2007), we decided to investigate whether the selective overexpression of 38A ncRNA would affect the formation of A $\beta$  x-42 and/or A $\beta$  x-40 species by measuring their relative amount in the medium of 38A-overexpressing SHSY5Y cells. As A $\beta$  processing might be altered by the transfection procedure, we first generated p38A and pMock permanently transfected cell lines (hereafter referred to as p38A-SHSY5Y and pMock-SHSY5Y, respectively). p38A-SHSY5Y cells, harboring extra copies of the 38A transcription unit with its natural PolIII type 3 promoter, exhibit a moderate overexpression of 38A ncRNA and, as a consequence, a 3.1-fold increased KCNIP4 Var IV/Var I ratio (Fig. 5, A and B). Culture media conditioned for 48 h with p38A-SHSY5Y and/or pMock-SHSY5Y cells were tested for their A $\beta$  peptide composition, showing that 38A significantly enhances the levels of A $\beta$  x-42 (up to 1.91-fold with respect to the pMock-transfected control), whereas its effect on the secretion of the more soluble A $\beta$  x-40 peptide is more modest (up to 1.4-fold with respect to the pMock-transfected control). These results indicate that the transcription of 38A and the concomitant synthesis of KCNIP4 Var IV change both quantitatively and qualitatively the A $\beta$  secretion, leading to an increased amount of the total A $\beta$  and, notably, to a concomitant variation of the A $\beta$  x-42/A $\beta$  x-40 ratio that could account for the altered ratio observed in

AD (Fig. 5 C). To further demonstrate the PolIII dependency (and the association with 38A) of the perturbation of A $\beta$  processing, a parallel experiment was performed in the presence of 20  $\mu$ M ML-60218; in this condition, the increment of both A $\beta$  x-42 and A $\beta$  x-40 was prevented, confirming the role of 38A PolIII-dependent expression in the impairment of A $\beta$  peptide production (Fig. 5 C). In this experiment, the specific inhibition of PolIII was confirmed, evidencing a decreased synthesis of PolIII-transcribed RNAs (5S ribosomal RNA [rRNA], 7SK RNA, and 38A RNA) and a concomitant unaffected expression of PolIII-dependent genes (cMyc and glyceraldehyde 3 phosphate dehydrogenase [GAPDH]; Fig. 5 D). Next, to discriminate whether the altered secretion of A $\beta$  in p38A-SHSY5Y cells has to be ascribed to a different level of APP processing or rather to the modulation of APP and/or PS2 synthesis, we measured their amount in the same experimental settings. Results showed that the levels of both APP and PS2 are not affected by the overexpression of 38A, either in the absence or in the presence of ML-60218, demonstrating that the perturbation of A $\beta$  promoted by 38A is specifically determined by the increase of APP processing (Fig. 5 E). This point was also confirmed by measuring A $\beta$  secretion in 38A-transfected APP-overexpressing HEK293 cells that stably overexpress APP. Indeed, although the amount of A $\beta$  secreted is considerably higher in these cells, the effects of 38A overexpression on APP processing recapitulate those obtained in SHSY5Y cells (Fig. S4 F).

We took advantage of a KCNIP4 Var IV-specific silencing RNA (hereafter referred to as siVar IV) to test the possible rescue of the 38A/KCNIP4 Var IV-dependent impairment of A $\beta$  secretion. To this aim, we transiently cotransfected p38A expressing together with siVar IV plasmid (or a scrambled siRNA-expressing plasmid as a control) and measured by real-time RT-PCR the amount of KCNIP4 Var I and Var IV mRNAs and the consequent variations of the secreted amyloid. Despite the overexpression of 38A, cells in which the Var IV was silenced expressed a significantly increased amount of the canonical Var I (up to a 7.84-fold increase with respect to pMock cells) and a decreased amount of Var IV (up to 0.35-fold of their original level; Fig. 5 F). In this condition, the secretion of A $\beta$  x-40 and A $\beta$  x-42 in the medium was reduced by 20 and 62%, respectively. As a consequence, the same samples exhibited a 27% reduced secretion of total amyloid and a 36% reduced A $\beta$  x-42/A $\beta$  x-40 ratio (Fig. 5 G). Thus, considering that the increased processing of APP induced by 38A can be reverted by the silencing of the alternative isoform IV, we hypothesized that 38A expression affects A $\beta$  secretion by promoting the synthesis of an alternative KCNIP4 protein form. Indeed, the same effect on A $\beta$  secretion driven by 38A overexpression can be replicated

(D) Immunofluorescence detection of KCNIP4 Var I and Var IV by splice variant-specific antibodies in pMock-transfected cells (M) and in 38A-overexpressing cells (38A). Bars, 100  $\mu$ m. (E) KCNIP4 Var I and PS2 signals in 38A-overexpressing cells. Bars, 100  $\mu$ m. (F) The KCNIP4 Var IV-specific antiserum does not evidence a colocalization of KCNIP4 and PS2. Bars, 100  $\mu$ m. (G) Western blot quantitative analysis of the PS1 and KChIP3 amount in Mock (M) and 38A-overexpressing (38A) cells. (H) Immunofluorescence detection of PS1 and KChIP3 in Mock (M) and 38A-overexpressing (38A) cells.  $\alpha$ -PS1,  $\alpha$ -anti-PS1;  $\alpha$ -KChIP3,  $\alpha$ -anti-KChIP3. (I) Immunofluorescence detection of PS2 and KChIP3 in Mock (M) and 38A-overexpressing (38A) cells. Bars, 100  $\mu$ m. The quantification of fluorescence signals shown in D–F, H, and I is reported in the corresponding histograms D'–F', H', and I'. The error bars (referred to the mean of 10 microscope fields) were not relevant enough to be visible in the graphs.  $\alpha$ -PS2,  $\alpha$ -anti-PS2.



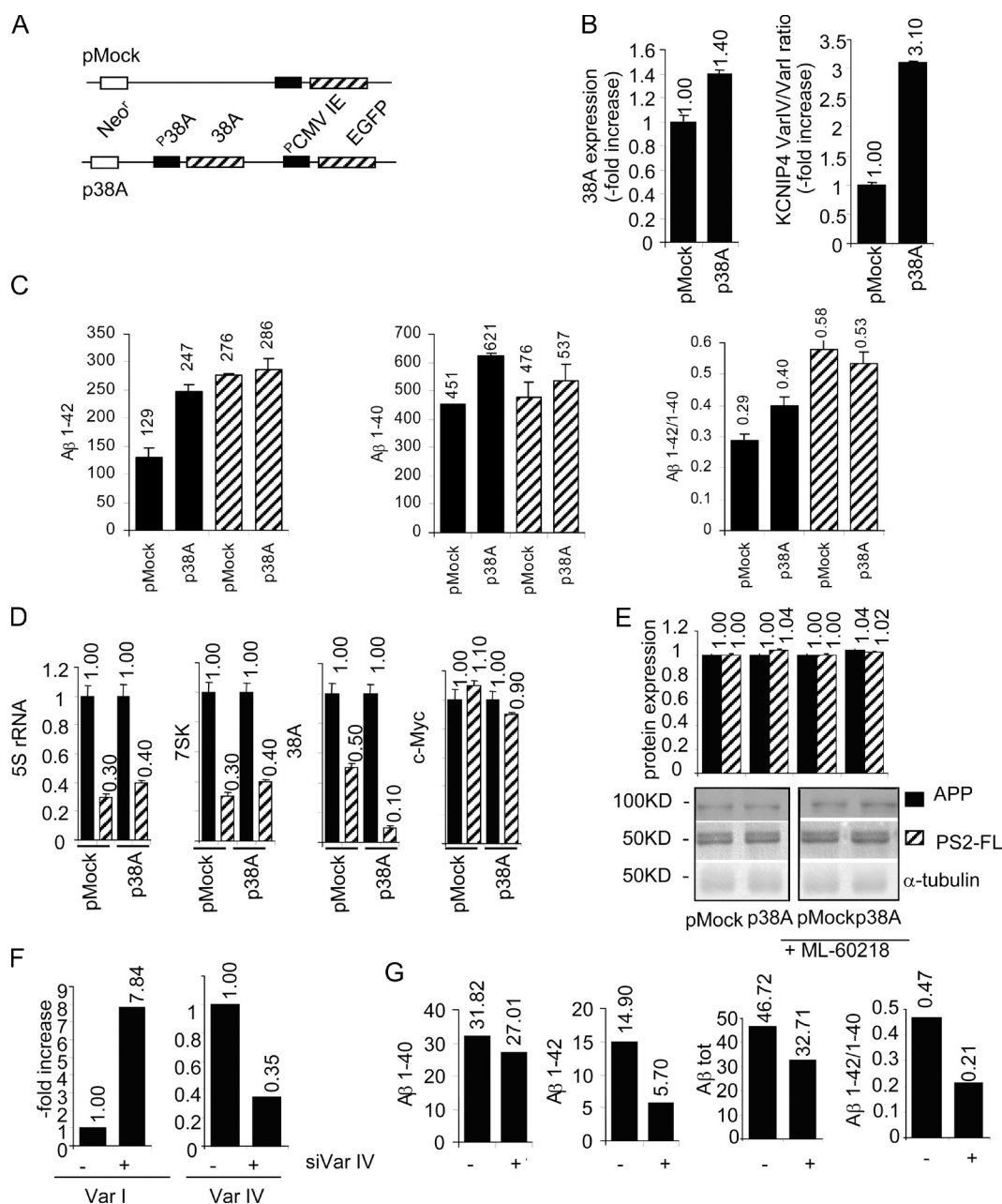


**Figure 5. 38A-induced perturbation of Aβ secretion.** (A) A schematic view of p38A and pMock plasmid constructs used to generate p38A-SHSY5Y and pMock-SHSY5Y permanently transfected cell lines. (B) Real-time RT-PCR quantitative determination of 38A expression and KCNIP4 splice variant ratio in p38A-SHSY5Y and pMock-SHSY5Y permanently transfected cell lines. (C) Increased β-amyloid secretion and perturbation of the Aβ x-42/Aβ x-40 ratio in 38A-overexpressing SHSY5Y cells. X axis, transfected plasmids; y axis, quantitative determination of Aβ (picograms/milliliter) secreted in the medium 48 h after medium replacement as determined by sandwich ELISA. The resulting Aβ x-42/Aβ x-40 ratio is reported. Striped bars, samples treated with ML-60218 PolIII-specific inhibitor; shaded bars, untreated cell samples. (D) A demonstration that PolIII transcription is specifically inhibited in ML-60218-treated cells, whereas it does not affect PolII activity. 5S rRNA, 7SK RNA, 38A, and c-Myc transcript abundances were detected by real-time RT-PCR in cells treated with ML-60218 and in untreated controls used as described in A. (E) Quantitative Western blotting analysis of APP and PS2 synthesis in pMock- and/or p38A-transfected cells in ML-60218-treated and -untreated conditions. All of the determinations were normalized to α-tubulin detections. (F and G) Suppression of the biological phenotype driven by the coexpression of 38A and KCNIP4 Var IV-specific silencing plasmid in SHSY5Y cells. Three independent determinations of Var IV decrease and the concomitant increase of Var I expression are shown together with the determinations of Aβ secretion in siVar IV silenced (+) with respect to cells transfected with a scrambled siRNA (-). The error bars were not relevant enough to be visible in the graphs; additional repetitions of the same experiment gave similar results (not depicted).

in cells that do not overexpress 38A by the transient overexpression of recombinant KCNIP4 Var IV (Fig. S3), thus suggesting a specific mechanism.

Altogether, the aforementioned results demonstrate that the overexpression of 38A leads to an impaired Aβ production

enhancing the secretion of the Aβ x-42 toxic isoform to the detriment of the more soluble Aβ x-40 isoform. Therefore, this cascade of reactions, triggered by the expression of a PolIII-dependent ncRNA, ultimately leads to the generation of a more neurotoxic composition of the secreted amyloid.



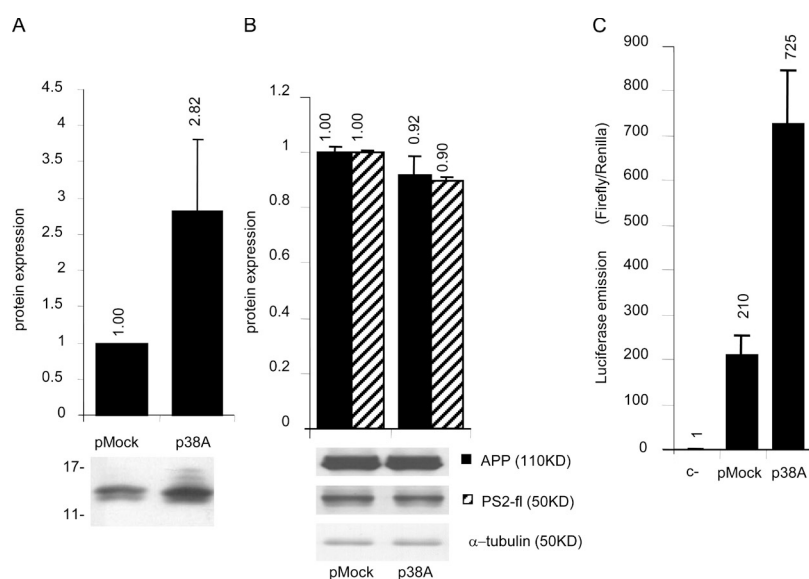


**Figure 6. Increased APP processing in 38A-overexpressing cells.** (A) Quantitative Western blotting analysis of APP C-terminal fragments in pMock- and/or p38A-transfected cells ( $P = 0.023$ , as the averaged result of five experiments). Error bars represent SD. (B) Quantitative determination of APP and PS2 synthesis in pMock- and/or p38A-transfected cells by Western blotting analysis. All of the determinations were normalized to  $\alpha$ -tubulin expression. Error bars represent SD. (C) Determination of APP processing by pGAL4-activated luciferase assay: c-, pLuc + pRL were transfected; pMock, pGAL4-APP + pGAL4-Luc + pMock + pRL were transfected; and p38A, pGAL4-APP + pGAL4-Luc + p38A + pRL were transfected.

### The enhanced synthesis of 38A affects A $\beta$ secretion, altering APP processing

To validate the hypothesis that 38A affects A $\beta$  secretion by altering APP processing, we tested the possible change of the C-terminal fragments profile generated by APP cleavage in 38A-overexpressing cells. To better detect these small C-terminal fragments in SDS-PAGE, we transiently transfected the 38A-expressing plasmid in HEK293-APP cells that harbor extra copies of the APP transcription unit. As shown in Fig. 6 A, 48 h after transfection, p38A-HEK293-APP cells are characterized by a significant increase of both  $\alpha$  and  $\beta$  APP C-terminal fragments detected at 10 and 12 kD, respectively, and generated by an increased processing of APP (2.82-fold).

To demonstrate that this phenomenon is not caused by the increased synthesis of APP (and/or PS2), we measured the levels of these proteins in p38A- and pMock-transfected HEK293-APP cells by Western blotting. Again, the levels of these proteins turned out to be unaffected by the expression of 38A (Fig. 6 B), further demonstrating that this ncRNA affects amyloid secretion by promoting APP processing by the means of a mechanism mediated by the synthesis of an alternative form of KCNIP4.

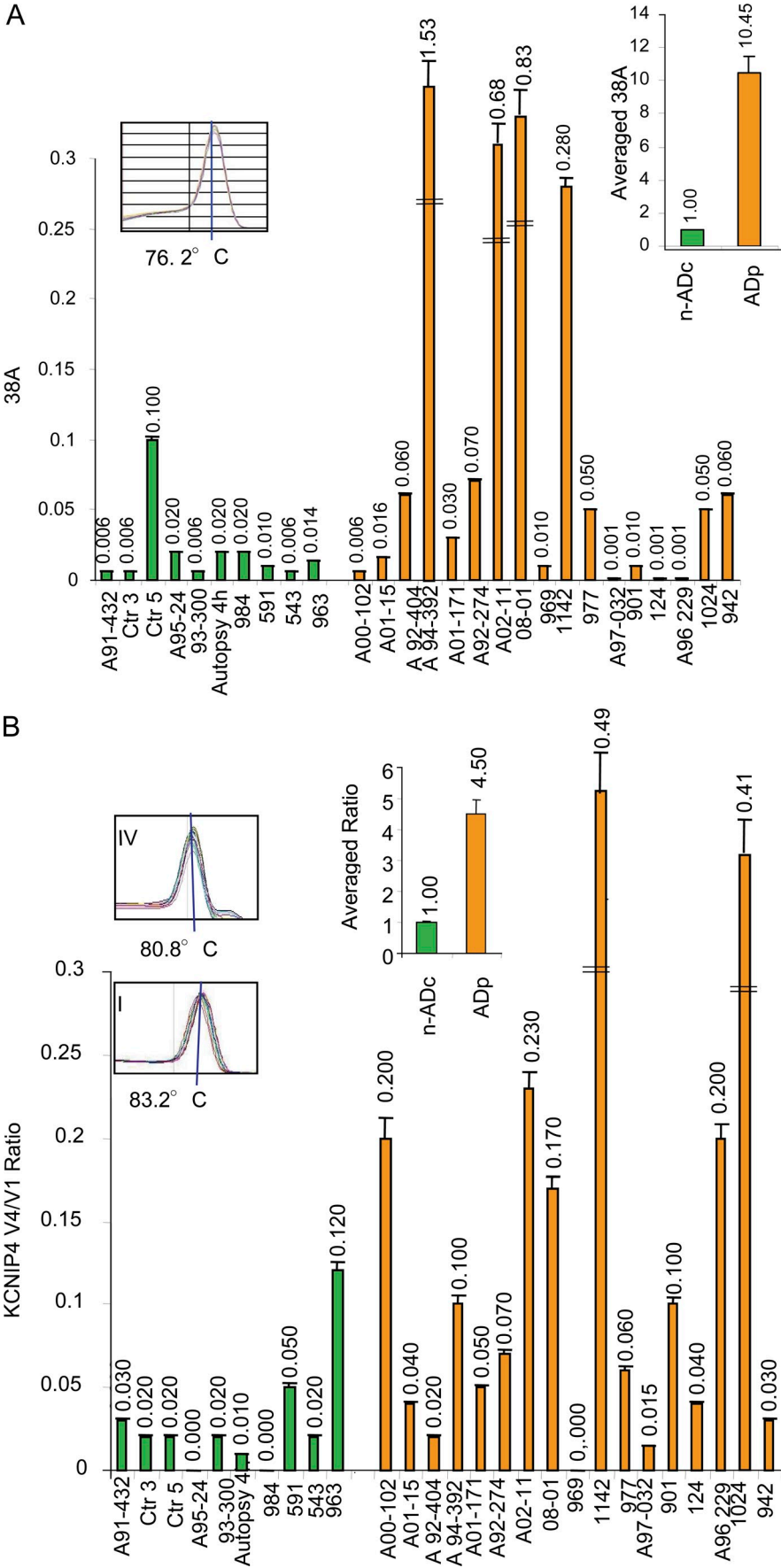
Additional evidence that the perturbation of A $\beta$  secretion is the consequence of an enhanced APP processing arose from an experiment in which SHSY5Y cells were transfected with different combinations of plasmids harboring (a) pGAL4-APP, a plasmid encoding for APP fused to the Gal4 activation domain (in this case, when APP is processed, the Gal4 activation activates the transcription of a cotransfected Gal4-dependent reporter gene); (b) pGAL4-Luc, encoding for the Gal4-dependent luciferase, thus activated by the processing of Gal4-APP; (c) p38A, encoding for 38A transcript driven by its natural promoter; and (d) pRL, encoding for Renilla luminescent protein as a normalizer. Results showed that in 38A-overexpressing cells, the processing of APP is significantly augmented, as revealed by an amplification of luciferase signal consequent to the release of the Gal4 activation domain (Fig. 6 C). Again, this demonstrates that the transcription of 38A ncRNA leads to a perturbation of APP processing that then leads to the increase of A $\beta$  secretion.

### AD cerebral cortices show a high level of 38A expression

As AD, the most common neurodegenerative disorder, is characterized by an aberrant A $\beta$  secretion, we hypothesized a possible overexpression of 38A in AD cases where it would play an active role in the onset and/or maintenance of pathological manifestations. First, we measured by quantitative real-time RT-PCR the levels of 38A RNA in postmortem cerebral cortex samples obtained from 17 AD patients and 10 non-AD control (nADc) individuals (Table S1). Results evidenced that AD cases tend to overexpress 38A (10.45-fold on average with respect to the nADc individuals), thus correlating the synthesis of this ncRNA with the AD phenotype. At present, we are not able to determine with statistic significance whether there is a correlation between 38A increment and a specific clinical or pathological marker. To date, we can only confirm that there is a significant positive correlation between expression of 38A and AD and a negative correlation with non-AD cases. This general conclusion is reinforced by inspection of some cases that might represent exceptions: (a) controls with higher levels of 38A are case 5, characterized by severe chronic obstructive pulmonary disease and likely hypoxic cerebral damage, and case 963, who was a cognitively normal subject but with a high load of angiopathy and a Braak stage III amyloid status; (b) the AD patient with the lowest 38A level is case 124, who is a familial AD case carrying mutated PS1 and in which PS1 loss/gain of function might exert a predominant role in comparison to 38A (Fig. 7 A). The unaltered transcription of the PolIII-transcribed 5S rRNA in the aforementioned samples indicated that the phenomenon is caused by the specific overexpression of 38A rather than a general increase of PolIII activity (unpublished data).

To confirm ex vivo that the overexpression of 38A in AD cases leads to the synthesis of KCNIP4 Var IV, we measured the relative amount of KCNIP4 Var I and Var IV in cortical extracts from AD and nADc individuals. Results confirmed that the overexpression of 38A in AD cases is associated with the alternative splicing shift of KCNIP4 that leads to the enrichment of Var IV to the detriment of the canonically expressed

**Figure 7. ncRNA expression and alternative splicing in AD cases.** (A) 38A expression in AD cases (orange bars) and nADc individuals (green bars) as determined by quantitative real-time RT-PCR. AD cases 124 and 1,024 have a familiar genetic origin. The amplification product dissociation curves unambiguously distinguish the RNAs of interest by peaks at specific temperatures (insets). Error bars represent SD of three independent real-time RT-PCR determinations. The averaged results are also reported. (B) Real-time RT-PCR quantitative detection of KCNIP4 splice variant synthesis in AD patients and nADc individuals. Results are reported as the splice variant ratio (KCNIP4 Var IV vs. Var I). Error bars represent SD of three independent real-time RT-PCR determinations. The averaged ratios are also reported. The dissociation curves (insets) show that the splice variants of interest are unambiguously distinguishable by peaks at specific temperatures. DSE, distal sequence element.



Var I (Fig. 7 B). Therefore, these results not only confirm *ex vivo* what was previously demonstrated *in vitro* but also associate the occurrence of this phenomenon with the most common neurodegenerative pathology, AD.

### Alternative 38A promoter variants exhibit peculiar transcriptional properties

To assess the relevance of KCNIP4 alternative splicing in neurodegeneration and with the final aim to identify 38A genetic variations associated with its unusual expression in AD samples, we sequenced the 38A genomic regions of 39 cerebral cortex samples from diseased and nondiseased cases. Results showed that, although the transcribed portion of 38A did not harbor major genetic alterations that might support its increased stability, 38A promoters contain recurrent genetic variations that could be responsible for its altered expression activation in AD cases. In detail, we isolated and cloned four different promoter variants, hereafter referred to as  $\alpha$ ,  $\beta$ ,  $\gamma$ , and  $\delta$  (Fig. 8 A and Table S2). Considering the  $\alpha$  variant as the wild type (wt) and  $\alpha/\alpha$  being the canonical wt genotype, we found a significant number of heterozygous genotypes (hereafter referred to as  $\alpha/\Sigma$ ) in the cerebral cortices that we analyzed ( $\Sigma$  being  $\beta$ ,  $\gamma$ , or  $\delta$  alleles). Interestingly, we found that in nADcs, the frequency of  $\alpha/\alpha$  homozygous and that of heterozygous genotypes was rather similar (47 and 53% of the cases, respectively); alternatively, this ratio is altered in AD samples in which the  $\alpha/\alpha$  genotype was associated with 27% of the individuals, whereas the  $\alpha/\Sigma$  heterozygous genotype was found in 73% of the diseased cases (Fig. 8 B). Although, because of the restricted number of samples in our collection ( $n = 39$ ), the different frequencies of promoter variants are not statistically significant to derive a detailed genetic determination of the impact of different promoters in the disease ( $\chi^2 = 1.63$ ,  $g = 1$ , and  $P = 80\%$ ), the genetic data obtained by this screening suggest that 38A overexpression is not an individual single determinant of the disease but rather is part of a multifactorial network of events. The transcriptional properties of 38A promoter variants were then investigated to identify an allele-specific regulation of transcription that might explain the increased frequency of the heterozygous haplotype among AD cases (Table S2). We found that the expression of the ncRNA is dependent on the PolIII promoter variant that drives its synthesis in a cell type-specific manner, leading to functionally active 38A ncRNA (Fig. S4). Altogether, these data demonstrate the occurrence of cell type-specific expression of 38A promoter variants that is compatible with a possible individual susceptibility to 38A transcriptional stimuli that might occur differentially in diseased and control cases.

### 38A expression is triggered by inflammatory stimuli

As the aforementioned findings demonstrate a role of 38A in brain function and, possibly, in neurodegeneration associated with AD, we focused on the investigation of possible biochemical stimuli that may promote 38A transcription in neurodegenerative disorders. Because several studies support the hypothesis of a relevant contribution of inflammatory stimuli to AD onset (Griffin et al., 1989; McGeer et al., 2006; Wyss-Coray, 2006), we tested the effect on 38A expression of treatments with

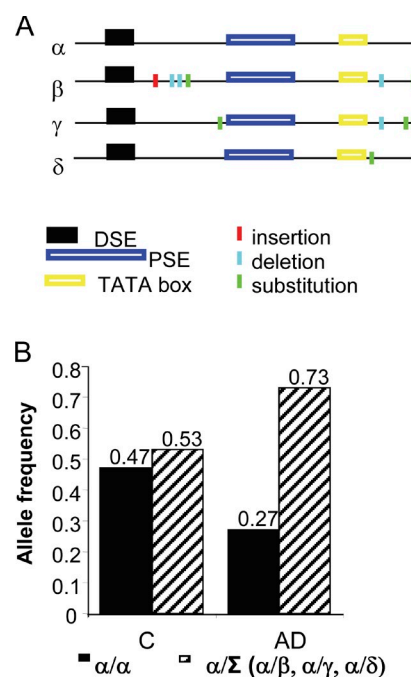


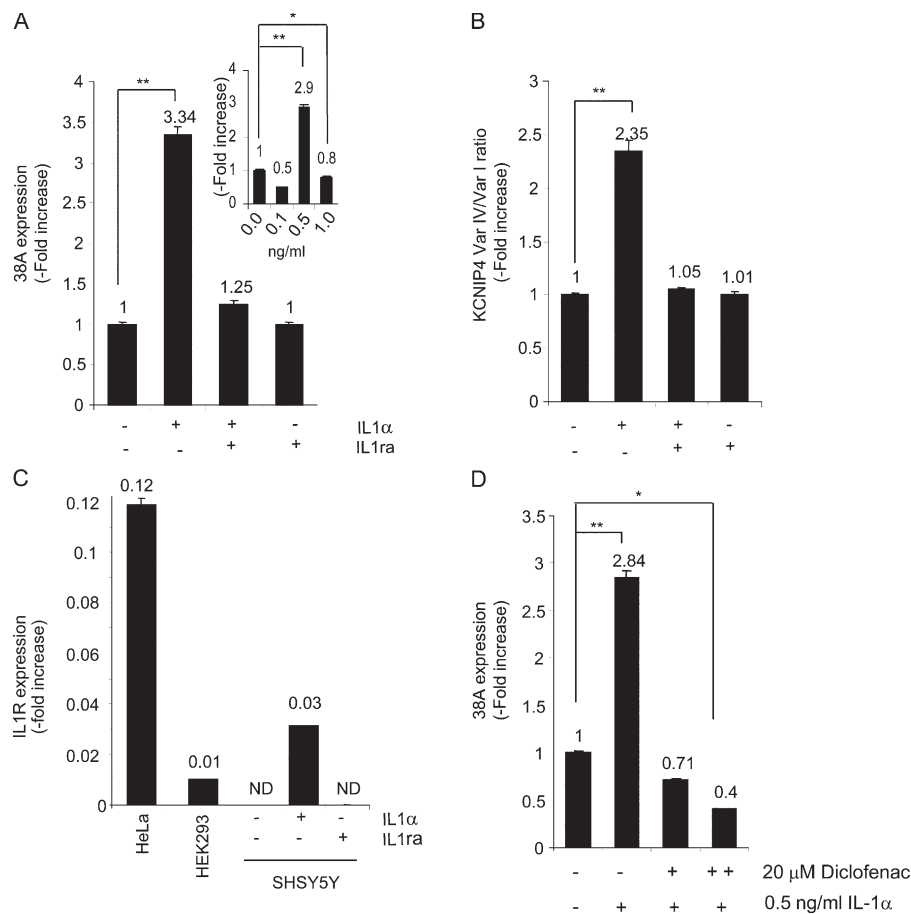
Figure 8. **38A promoter variants analysis.** (A) A schematic representation of 38A promoter genetic variants. (B) Relative frequencies of genetic configurations.  $\alpha/\alpha$  genetic configuration versus  $\alpha/\Sigma$  genetic configuration in AD cases and in nADcs (C).

different proinflammatory molecules in SHSY5Y cells. We found that 12 h after treatment, 0.5 ng/ml IL1- $\alpha$  strongly up-regulates 38A expression, whereas the addition of IL1 receptor antagonist (IL1ra, a natural inhibitor of IL1- $\alpha$  proinflammatory effect) prevents the IL1- $\alpha$ -dependent increase of 38A transcription, demonstrating further the specificity of IL1- $\alpha$  action (Fig. 9, A and B). We then measured the expression of IL1- $\alpha$  receptor by real-time RT-PCR in the same samples. IL1- $\alpha$  receptor expression was found to be abundant in HeLa and, at a lesser extent in HEK293 cells, not detected in SHSY5Y-untreated cells, where it was induced by the treatment with the inflammatory agent, supporting the effects of IL1- $\alpha$  on A $\beta$  processing described in this paper (Fig. 9 C). Next, we repeated the induction of 38A expression with IL1- $\alpha$  in samples previously treated with Diclofenac to test a possible protective effect of a nonsteroidal antiinflammatory drug on 38A activation. Under these conditions, IL1- $\alpha$ -dependent 38A activation was abolished, thus demonstrating that the inhibition of the COX-2 (Cyclooxygenase-2)-dependent inflammatory cascade is sufficient to prevent IL1- $\alpha$ -dependent up-regulation of 38A and its possible detrimental consequences (Fig. 9 D). Altogether, these results demonstrate that 38A expression is induced by IL1- $\alpha$  and that the harmful effects of its activation (such as the increased processing of A $\beta$  and the impairment of A-type potassium current) might be triggered *in vivo* by this inflammatory stimulus.

## Discussion

In this paper, we propose that a newly identified ncRNA molecule transcribed by RNA PolIII, 38A, controls the splicing process of a protein-coding gene, KCNIP4, and that this mechanism

**Figure 9. Modulation of 38A promoter activity by inflammatory and antiinflammatory agents.** (A) Induction by IL1- $\alpha$  treatment and recovery by IL1ra of 38A expression. The results were normalized to the untreated samples. The effects of different concentrations of IL1- $\alpha$  treatment on 38A expression are shown in the inset. (B) KCNIP4 splice variant shift induction and prevention by IL1- $\alpha$  and IL1ra, respectively. (C) Induction by IL1- $\alpha$  treatment of IL1R expression in SHSY5Y cells. HeLa and HEK293 cells were used as positive controls. (D) Inhibition of IL1- $\alpha$ -induced 38A overexpression by Diclofenac treatment. Experiments were performed in triplicate and repeated three times. Data are reported as mean values  $\pm$  SD. Statistical significance was examined using the unpaired Student's *t* test. \* and \*\* indicate statistical significance at  $P < 0.05$  and  $0.01$ , respectively.



of cogene/gene regulation is at the root of a novel PolIII-dependent gene expression regulatory mechanism that is of relevant interest in brain physiology and/or pathology. In detail, this work demonstrates that (a) after the induction by an inflammatory stimulus that promotes its transcription, 38A drives the splicing of KCNIP4 pre-mRNA to the synthesis of the alternative protein Var IV, which differs from the canonical KCNIP4 for its N-terminal portion; (b) as a consequence, KCNIP4 loses the ability to physically interact with PS2, a component of the  $\gamma$ -secretase complex; (c) this lack of interaction leads to a general increase of APP processing and A $\beta$  secretion and to a specific alteration of the A $\beta$  x-42/A $\beta$  x-40 ratio, favoring the production of the insoluble, more toxic A $\beta$  x-42 species; (d) besides this effect on A $\beta$  production, 38A activation and the subsequent synthesis of KCNIP4 Var IV lead to the concomitant blockade of the fast kinetics of potassium channels with significant inhibition of their A-type current (because this current plays an important role in the process of LTP associated with brain plasticity and memory, this effect is of particular relevance, as it suggests an additional detrimental role of 38A with respect to brain physiology and thus may account for a novel contribution of 38A to AD and to the symptoms associated with neurodegenerative processes); (e) 38A is significantly up-regulated in cerebral cortex samples of AD individuals in which the concomitant alternative splicing of KCNIP4 is observed; (f) the 38A promoter was found to occur in four allelic variants, of which the wt homozygous  $\alpha/\alpha$  is more frequently associated with non-AD individuals,

whereas the heterozygous genetic configurations are more frequently associated with the AD individuals; and (g) the alternative promoter variants appear to be expressed in a cell type-specific manner so that in each cell type, the 38A expression is allele specific. This finding suggests that, in specific conditions, individuals harboring the  $\alpha$ ,  $\beta$ ,  $\gamma$ , or  $\delta$  allele might be differentially prone to 38A activation. The fact that the activation of 38A and of the subsequent cascade of reactions is induced specifically by IL1- $\alpha$  suggests that the active synthesis of this ncRNA in AD cortices may be promoted by a prolonged inflammation that would thus anticipate the neurodegenerative manifestations. In this context, the present work provides a mechanistic link between inflammation and AD, supporting the hypothesis that protracted inflammatory stimuli might contribute to its onset and/or maintenance and indicating the possible use of antiinflammatory drugs to prevent AD.

In light of the aforementioned findings, we propose a model that is in line with the amyloid hypothesis and proposes a series of inflammation-dependent early events that ultimately lead to altered amyloid production and to the impairment of a voltage-dependent current contributing to the excitatory properties to neurons (Fig. 10). Although at present it is not clear whether 38A is essential for AD onset or is rather part of a pathological condition of the brain that occurs in numerous neurodegenerative disorders, this model provides a novel way to investigate neurodegenerations and brain function based on an alternative cascade of reactions unexpectedly controlled by a PolIII-transcribed ncRNA.



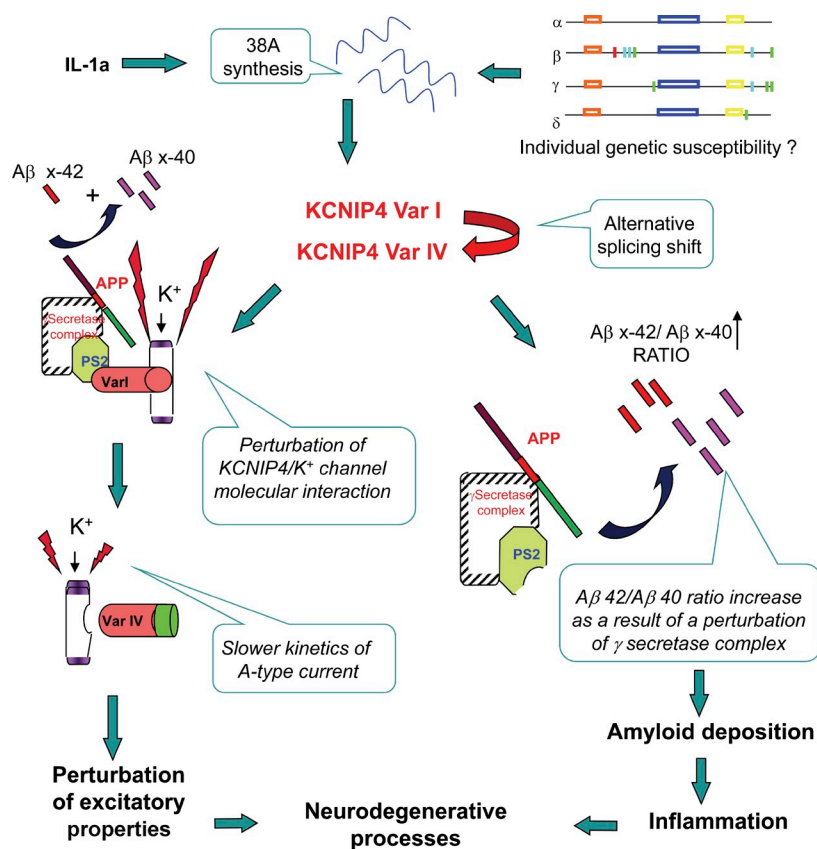


Figure 10. A schematic model of the possible contribution of the 38A cogene to neurodegeneration.

Indeed, although the genetic analysis of 38A alleles in AD and controls does not support its role in the disease as a single determinant element, the unbalanced frequency of its promoter configurations suggests its contribution to the disease in association with other elements. Moreover, the cell type-specific regulation of 38A suggests the involvement of still elusive PolIII-specific transcription factors whose identification might reveal new genes associated with sporadic AD. In this context, a detailed investigation of the transcriptional properties of 38A promoter variants might allow us to identify possible AD risk factors and/or druglike compounds able to decrease the amyloid production via 38A transcription inhibition. In conclusion, this work provides novel information of particular relevance, as (a) it proposes a novel mechanism by which the alternative splicing can be involved in brain pathologies, (b) it proposes a role for PolIII-transcribed ncRNAs in orchestrating the regulation of a mosaic of alternative protein forms in different tissues or cell conditions, and (c) it indicates new specific genomic loci to which genetic variations that account for pathological manifestations might be mapped.

## Materials and methods

### In vitro transcription

Transcription reactions were performed in the presence of 2 µg of template DNA and 100 µg HeLa cell nuclear extract supplemented with 50 ng recombinant human TATA-binding protein as follows: 5 mM creatine phosphate, 70 mM KCl, 5 mM MgCl<sub>2</sub>, 20 mM Tris/HCl, pH 8, 1 mM DTT, 2 µg/ml α-amanitin, 0.5 mM CTP, ATP, and GTP, 25 µM/10 µCi UTP/α-[<sup>32</sup>P]UTP, 10 U SUPERase IN (Invitrogen), and 10% glycerol (vol/vol) for 1 h at 30°C. For primer extension analysis, the purified transcripts were resuspended

in the presence of 0.5 mM deoxynucleotide triphosphates and 1 pmol of specific 5' end-radiolabeled probe. A mixture providing 50 mM Tris/HCl, pH 8, 75 mM KCl, 3 mM MgCl<sub>2</sub>, 5 mM DTT, 10 U SUPERase IN, and 200 U Superscript III reverse transcription (Invitrogen) was then added, and the reactions were incubated for 1 h at 60°C, precipitated with ammonium acetate, and gel fractionated. To construct templates for in vitro transcription, a 38A fragment was amplified from human genomic DNA and cloned into pGEM-Teasy vector (Promega) by using the primers 5'-TAATAA-CAACATATCTGAAAAAGACGC-3' and 5'-TTCAGGGTGCTCTGTGG-TACC-3'. The inserts were then subcloned into pNEB193 vector. The fusion 38A/7SK DNA fragment was obtained by amplifying the 7SK coding region with a primer containing the 38A upstream sequence from -68 to -27 bp. The hybrid product was cloned into pNEB193 vector.

### ChIP

ChIP and radiolabeled PCR analysis of immunoprecipitated and input DNA were performed as previously described (Wang et al., 2005). The following antibodies were used: anti-SNAP43 (a gift from W. Henry, Michigan State University, East Lansing, MI; Hirsch et al., 2004), anti-Brf2/TFIIIB50, and anti-RPC39 (a gift from M. Teichmann, Institut Européen de Chimie et Biologie, Bordeaux, France). The following oligonucleotide primer pairs were used: 5'-AGGTCATCCCTGAGCTGAAC-3' and 5'-CCA-CCTGGTGCTCAGTGTAG-3' for GAPDH; 5'-TAATAACAACATATCTGAA-AAAGACGC-3' and 5'-GTGTCTTCTTCAACTTTTTATC-3' for 38A; and 5'-GTACAAAATACGTGACGTAGAAAG-3' and 5'-GGTGTTCGT-CCTTCCACAAG-3' for the U6 gene. PCR products were resolved on 6% polyacrylamide-1X Tris-borate-EDTA gels, and PCR signals were visualized and quantified by Molecular Imager FX (Bio-Rad Laboratories). To estimate the specific enrichment of target DNA regions, the ratio of each PolIII-specific product to that of a PolII-transcribed gene (GAPDH exon 2) in the immunoprecipitations was determined after normalization for amplification efficiency.

### Cell culture, transfection, and luciferase assay

HeLa, SHSY5Y, IMR32, and SK-N-BE cells were transfected with pEGFP-N1 constructs using polyethylenimine (PEI; P3143; 1 µg DNA/2.5 µl PEI 10 mM; Sigma-Aldrich). G418 (Geneticin) was used as a means of selection up to 1,000 µg/ml until resistant clones were identified. Clones were then preserved in 200 µg/ml G418. The luciferase-based promoter activity assay

(a gift from T. Russo, University of Naples-Federico II, Naples, Italy) was performed using the dual luciferase reporter assay system (Promega) according to the manufacturer's protocol. ML-60218 (EMD) was added to the medium at the concentration of 20  $\mu$ M 26 h before the assay.

### DNA sequencing

All of the DNA samples were sequenced using the BigDye Terminator DNA sequencing kit (Applied Biosystems) according to the manufacturer's instructions.

### Real-time quantitative RT-PCR analysis

Total RNAs were extracted using TRIzol reagent (Invitrogen), subjected to reverse transcription by the Omniscript RT kit (QIAGEN), and measured by real-time quantitative RT-PCR using the PE ABI PRISM 7700 Sequence Detection System and Sybr green method (PerkinElmer). The sequences of 38A forward and reverse primers were 5'-CTATCAAAATTTCAAGGATATGCATCA-3' and 5'-GATGCCTCAAGCTTTGTTTGC-3'. The sequences of KCNIP4 (Var I) forward and reverse primers were 5'-ATGAAGCTCTTGCCCTGCTC-3' and 5'-CGGTGGCCATCTCCAGTT-3'. The sequences of KCNIP4 (Var IV) forward and reverse primers were 5'-TGGAACAGTTGGGCTGATTG-3' and 5'-CGGTGGCCATCTCCAGTT-3'. For endogenous control, the expression of the GAPDH gene was examined. The sequences for human GAPDH primers were 5'-GAAGGTGAAGGTGCGAGTC-3' and 5'-GAAGATGGTGATGGGATTTC-3'. The sequences for human 5s rRNA primers were 5'-TACGGCCATACCACCCTGAA-3' and 5'-GCGGTCTCCCATCCCAAGTAC-3'. The sequences for human 7SK RNA primers were 5'-AGGACCGGTCTTCGGTCAA-3' and 5'-TCATTGGATGTGTCTGCAGTCT-3'. The sequences for human c-Myc primers were 5'-CGTCTCCACACATCAGCATAA-3' and 5'-GACACTGTCCAACCTGACCCTCTT-3'.

### Immunofluorescence detection

SHSY5Y cells were grown overnight on culture slides and then transfected with pcr2.1-38A (or pcr2.1 as a control) using PEI. 48 h after transfection, the cells were washed in PBS, fixed for 10 min with 10% buffered formalin, and blocked for 15 min with 3% BSA in PBS. Cells were subsequently incubated with primary antibodies overnight at 4°C in 0.5% BSA in PBS. The day after, the cells were labeled with secondary antibodies for 45 min in 0.5% BSA/PBS solution. (Only the slides for PS1 and the downstream regulatory element antagonist modulator [DREAM] after the incubation with primary and secondary antibody for DREAM were permeabilized for 5 min with 0.25% Triton X-100 in PBS, blocked for 5 min with 3% BSA in PBS, and incubated with antibody for PS1 that recognized the C terminus of the protein and with the secondary antibody. Because DREAM and PS1 were both produced in rabbit, a control without primary antibody for PS1 was also performed to verify the absence of reaction between intracellular DREAM and secondary anti-rabbit rhodamine-TRITC.) Cells were then incubated with DAPI for 5 min and mounted with Mowiol (Invitrogen). Immunostained cells were observed with the appropriate filters on a microscope (Axiovert 200 M; Carl Zeiss) with a 40 $\times$ /0.75 Plan Neofluar objective and captured with a camera (Axiocam HR; Carl Zeiss) at the same adjustments of laser intensity and photomultiplier sensitivity using AxioVision Release 4.8.1 software (Carl Zeiss). Antibodies used were mouse monoclonal anti-PS2 H-76 (1:50; sc-7861; Santa Cruz Biotechnology, Inc.), rabbit polyclonal anti-KCNIP4 Var IV (1:200; raised against the sequence KLLEQFLIEAGLEC), goat polyclonal anti-KCNIP4-N14 (1:200; sc-46381; Santa Cruz Biotechnology, Inc.), rabbit polyclonal anti-DREAM FL-214 (1:200; sc-9142; Santa Cruz Biotechnology, Inc.), and rabbit polyclonal anti-PS1 S182 (1:100; P 7854; Sigma-Aldrich). Secondary antibodies used were anti-goat rhodamine-TRITC (1:200; Jackson ImmunoResearch Laboratories, Inc.) for KCNIP4-N14, anti-rabbit rhodamine-TRITC (1:200; Jackson ImmunoResearch Laboratories, Inc.) for KCNIP4 Var IV and PS1, anti-mouse FITC (1:200; Jackson ImmunoResearch Laboratories, Inc.) for PS2, anti-rabbit FITC (1:200; Jackson ImmunoResearch Laboratories, Inc.) for DREAM and KCNIP4 Var IV, and anti-mouse rhodamine-TRITC (1:200) for PS2 (Jackson ImmunoResearch Laboratories, Inc.).

### Detection of fast inactivation of K<sup>+</sup> channels

Currents were measured with a standard whole cell patch clamp technique using an EPC-7 amplifier (D-6100; Darmstadt List Medical). Patch pipettes were prepared from borosilicate glass capillaries using a P-30 puller (Sutter Instrument). Membrane potential and ionic currents were measured in the standard whole cell patch clamp configuration. Ionic currents were recorded with a Labmaster D/A, A/D converter driven by pClamp software (Axon Instruments). Analysis was performed with pClamp and SigmaPlot software (Jandel Scientific). The standard external solution contained 135 mM NaCl, 5.4 mM KCl, 1.8 mM CaCl<sub>2</sub>, 1 mM MgCl<sub>2</sub>, 5 mM Hepes,

10 mM glucose, and 300 nM tetrodotoxin; pH was adjusted to 7.4 using NaOH. The pipette filling (internal) solution contained 142 mM KCl, 10 mM Hepes, 2 mM EGTA, 4 mM MgCl<sub>2</sub>, and 3 mM ATP. The pH was adjusted to 7.3 with Tris base. All chemicals were purchased from Sigma-Aldrich. The external solution was applied to the cell bath by steady perfusion (~3 ml/min of gravity flow). The potassium currents were elicited from a holding potential of -80 mV by depolarizing voltage pulses ranging from -40 to 60 mV at 20-mV increments. The depolarizing voltage pulses of 200-ms duration were applied every 5 s. A best fit exponential function was used to determine the time constant of the current inactivation.

### A $\beta$ detection in SHSY5Y permanently transfected cells

The amount of secreted A $\beta$  x-40 and A $\beta$  x-42 in the media of 38A permanently transfected SHSY5Y cells were evaluated by sandwich ELISA (IBL-Japan) according to the manufacturer. Because the overexpression of 38A did not alter the proliferation rate of SHSY5Y, the equal number of cells seeded in 38A-overexpressing and/or control cells remained constant during the 48 h of conditioning of the medium by the cells. Notwithstanding, the results were normalized either to the cell number as well as to the protein content of the cell culture showing no variations in the two cells.

### Western blot analysis

The proteins were quantified using a commercial protein quantification kit (Protein Assay; Bio-Rad Laboratories) according to the manufacturer's instructions. The samples were subsequently analyzed by 10% SDS-PAGE and transferred to a nitrocellulose membrane (GE Healthcare). The membranes were initially blocked by an incubation of 2 h in TBST-Tween 20 (TBST; 50 mM Tris-HCl, 150 mM NaCl, pH 7.5, and 0.05% Tween 20) containing 5% nonfat dried milk. The blots were incubated for 1 h with the appropriate primary antibodies: goat polyclonal anti-KChIP4 L14 (sc-46380; 1:100), goat polyclonal anti-KChIP4 (N14; sc-46381; 1:100), rabbit polyclonal anti-PS2 H-76 (sc-7861; 1:200; Santa Cruz Biotechnology, Inc.), rabbit polyclonal anti- $\beta$ -APP (clone CT695; 1:250; Invitrogen), rabbit polyclonal anti-DREAM FL-214 (sc-9142; 1:200; Santa Cruz Biotechnology, Inc.), and anti-PS1 S182 (1:5,000; P 7854; Sigma-Aldrich).

To normalize the protein levels of KCNIP4, APP, and PS2, PS1 Western blot membranes were stripped with Restore Western blot stripping reagent (Thermo Fisher Scientific) and then probed with a monoclonal antibody against  $\alpha$ -tubulin (clone B-5-1-2; T 5168; 1:2,000; Sigma-Aldrich). APP C-terminal fragments were analyzed by 10–18% Tris-Tricine SDS-PAGE followed by Western blotting and immunorevelation with IgGs. All primary antibodies were then diluted in 0.1% Na<sub>2</sub>S<sub>2</sub>O<sub>5</sub> and 1% BSA-TBS. After washing with TBST, membranes were incubated with peroxidase-conjugated secondary antibodies anti-mouse IgGs (1:12,000; A 0168; Sigma-Aldrich), anti-rabbit IgGs (A 0545; 1:16,000; Sigma-Aldrich), and anti-goat IgGs (805-035-180; Jackson ImmunoResearch Laboratories, Inc.) for 1 h at RT. After washing, the reactive bands were revealed with ECL (GE Healthcare). The densitometric analysis of protein bands was performed taking advantage of the ImageJ software system (National Institutes of Health).

### Immunoprecipitation

SHSY5Y cells were grown overnight and transiently transfected with p38A and/or pMock. 48 h after transfection, the cells were rinsed once with ice-cold PBS, pH 8, and incubated with 1 mM of chemical cross-linking dithio-bis-succinimidyl dipropionate (Thermo Fisher Scientific) for 30 min at 25°C. The reactions were then quenched in 50 mM Tris-HCl, pH 7.5, for 15 min. Cells were then scraped in 50 mM Tris-HCl, pH 7.5, 150 mM NaCl, 1% Triton, and 1 mM PMSF with the addition of a protease inhibitor cocktail (mini-complete; Roche) and passed five times through a 27-gauge needle; samples were centrifugated at 11,000 g for 15 min, and the supernatants were quantified (Thermo Fisher Scientific) and used for the immunoprecipitation. The solubilized samples were precleared with protein G-conjugated agarose (Pharmacia) for 1 h at 4°C, reacted with a primary goat polyclonal antibody raised against a peptide mapping within a KCNIP4 internal region (KChIP4 L-14) overnight followed by incubation with 20  $\mu$ l of protein G-agarose for 1 h at 4°C. After three washing steps in ice-cold PBS, pH 8, samples were boiled for 5 min in Laemmli sample buffer supplemented by 40 mM DTT and loaded on an SDS-PAGE gel.

### KCNIP4 Var IV down-regulation

For KCNIP4 Var IV down-regulation, an engineered microRNA-KCNIP4V4, 5'-TGCTGTATCATTTCAAGCCCTTCCAAGTTTGGCCACTGACTGACTTG-3', was designed against the 5'-specific sequence following the BLOCK-iT PolII miR RNAi Expression Vector kit guidelines (Invitrogen) and cloned in the pCEG vector. Control experiments were performed using either pCEG alone

or the pCMMP retroviral GFP vectors. SHSY5Y wt cells were cotransfected with a construct expressing 38A (pcr2.1-38A or pcr2.1 as a control) and microRNA-KCNIP4V4 (or a scrambled negative microRNA control) with microporator (DigitalBio) at 1,400 V, 20 ms, and one pulse. 48 h after transfection, RNA extraction and amyloid detection on conditioned media were performed. For KCNIP4 Var IV down-regulation, SHSY5Y cells were transfected with a construct expressing the KCNIP4 Var IV and KCNIP4-KIS domain, provided by P. Liang and K. Wang (Neuroscience Research Institute, Peking University Health Science Center, Beijing, China).

## Statistics

Experiments were performed in triplicate and repeated three times. Data are reported as mean values  $\pm$  SD, and statistical significance was examined using the unpaired Student's *t* test. In the figures, \* and \*\* indicate statistical significance at *P* < 0.05 and 0.01, respectively.

## Human brain samples

Frontal and temporal cortices from AD (clinical history of disease; pathological diagnosis according to the Consortium to Establish a Registry for Alzheimer's Disease criteria) and control cases (AD excluded by clinical history and by immunohistochemical analysis) derive from P. Gambetti (Case Western Reserve University, Cleveland, OH) and C. Hulette and the Joseph and Kathleen Bryan Alzheimer's Disease Research Center (Duke University Medical Center, Durham, NC). Patient characteristics are summarized in Table S1.

## Online supplemental material

Fig. S1 shows the schematic view and sequences of KCNIP4 alternatively spliced protein variants (A) and the schematic view of KCNIP4 alternatively spliced RNAs (B). Fig. S2 shows PolIII dependency of 38A-driven alternative splicing shift, and Fig. S3 shows that the alternative splicing of KCNIP4 Var IV plays a key role in the impairment of A $\beta$  processing. Fig. S4 shows the transcriptional activity and amyloid secretion in SHSY5Y cells overexpressing 38A under the control of different 38A promoter variants. Table S1 shows cerebral cortex samples, and Table S2 shows the relative frequencies of 38A promoter genetic variants in Alzheimer's-diseased cerebral cortices and nADc individuals. Online supplemental material is available at <http://www.jcb.org/cgi/content/full/jcb.201011053/DC1>.

Dr. Ping Liang and Dr. Kewei Wang are gratefully acknowledged for the KCNIP4 Var IV and KCNIP4-KIS domain expression plasmids. We thank Dr. Gregory Hannon (Cold Spring Harbor Laboratory, New York, NY) for providing the pSHAG-ff1 plasmid. We thank W. Henry for anti-SNAP43 antibodies and Martin Teichmann for anti-Brf2 and anti-RPC39 antibodies and recombinant human TATA-binding protein. The pGal4-APP luciferase assay reagents were a gift from Tommaso Russo. We thank Luciano D'Adamio (Albert Einstein College of Medicine, New York, NY) for HEK293-APP cells. We gratefully acknowledge Professor P. Gambetti, Professor C. Hulette, and the Joseph and Kathleen Bryan Alzheimer's Disease Research Center for providing brain tissues.

R. Cancedda was supported by the Italian Ministry of University and Research (MIUR; 2007 International Basic Research Investment Fund Program). G. Dieci was supported by Fondazione Cariparma (2010 grant program) and by the Italian Ministry of Education, University, and Research (MIUR, Projects of Relevant National Interest [PRIN] Program). A. Pagano was supported by the MIUR (2007 PRIN Program prot. 2007945BZN), the Associazione Italiana Ricerca sul Cancro (2009 Program no. IG9378), and by the Associazione Italiana per la Lotta al Neuroblastoma.

Submitted: 9 November 2010

Accepted: 2 May 2011

## References

Angulo, E., V. Noé, V. Casadó, J. Mallol, T. Gomez-Isla, C. Lluís, I. Ferrer, C.J. Ciudad, and R. Franco. 2004. Up-regulation of the Kv3.4 potassium channel subunit in early stages of Alzheimer's disease. *J. Neurochem.* 91:547–557. doi:10.1111/j.1471-4159.2004.02771.x

Baranaskas, G. 2004. Cell-type-specific splicing of KCHIP4 mRNA correlates with slower kinetics of A-type current. *Eur. J. Neurosci.* 20:385–391. doi:10.1111/j.1460-9568.2004.03494.x

Bentahir, M., O. Nyabi, J. Verhamme, A. Tolia, K. Horré, J. Wiltfang, H. Esselmann, and B. De Strooper. 2006. Presenilin clinical mutations can affect gamma-secretase activity by different mechanisms. *J. Neurochem.* 96:732–742. doi:10.1111/j.1471-4159.2005.03578.x

Biedler, J.L., and B.A. Spengler. 1976. Metaphase chromosome anomaly: association with drug resistance and cell-specific products. *Science.* 191:185–187. doi:10.1126/science.942798

Biedler, J.L., L. Helson, and B.A. Spengler. 1973. Morphology and growth, tumorigenicity, and cytogenetics of human neuroblastoma cells in continuous culture. *Cancer Res.* 33:2643–2652.

Boland, L.M., M. Jiang, S.Y. Lee, S.C. Fahrenkrug, M.T. Harrett, and S.M. O'Grady. 2003. Functional properties of a brain-specific NH2-terminally spliced modulator of Kv4 channels. *Am. J. Physiol. Cell Physiol.* 285:C161–C170.

Buxbaum, J.D., E.K. Choi, Y. Luo, C. Lilliehook, A.C. Crowley, D.E. Merriam, and W. Wasco. 1998. Calsenilin: a calcium-binding protein that interacts with the presenilins and regulates the levels of a presenilin fragment. *Nat. Med.* 4:1177–1181. doi:10.1038/2673

Castelnuovo, M., S. Massone, R. Tasso, G. Fiorino, M. Gatti, M. Robello, E. Gatta, A. Berger, K. Strub, T. Florio, et al. 2010. An Alu-like RNA promotes cell differentiation and reduces malignancy of human neuroblastoma cells. *FASEB J.* 24:4033–4046. doi:10.1096/fj.10-157032

Decher, N., B. Pirard, F. Bundis, S. Peukert, K.H. Baringhaus, A.E. Busch, K. Steinmeyer, and M.C. Sanguinetti. 2004. Molecular basis for Kv1.5 channel block: conservation of drug binding sites among voltage-gated K<sup>+</sup> channels. *J. Biol. Chem.* 279:394–400. doi:10.1074/jbc.M307411200

Deng, X.Y., F. Cai, K. Xia, Q. Pan, Z.G. Long, L.Q. Wu, D.S. Liang, H.P. Dai, Z.H. Zhang, and J.H. Xia. 2005. Identification of the alternative promoters of the KCHIP4 subfamily. *Acta Biochim. Biophys. Sin. (Shanghai).* 37:241–247. doi:10.1111/j.1745-7270.2005.00034.x

Dieci, G., G. Fiorino, M. Castelnuovo, M. Teichmann, and A. Pagano. 2007. The expanding RNA polymerase III transcriptome. *Trends Genet.* 23:614–622. doi:10.1016/j.tig.2007.09.001

Etcheberrigaray, R., E. Ito, K. Oka, B. Tofel-Grehl, G.E. Gibson, and D.L. Alkon. 1993. Potassium channel dysfunction in fibroblasts identifies patients with Alzheimer disease. *Proc. Natl. Acad. Sci. USA.* 90:8209–8213. doi:10.1073/pnas.90.17.8209

Griffin, W.S., L.C. Stanley, C. Ling, L. White, V. MacLeod, L.J. Perrot, C.L. White III, and C. Araoz. 1989. Brain interleukin 1 and S-100 immunoreactivity are elevated in Down syndrome and Alzheimer disease. *Proc. Natl. Acad. Sci. USA.* 86:7611–7615. doi:10.1073/pnas.86.19.7611

Haass, C., and D.J. Selkoe. 2007. Soluble protein oligomers in neurodegeneration: lessons from the Alzheimer's amyloid beta-peptide. *Nat. Rev. Mol. Cell Biol.* 8:101–112. doi:10.1038/nrm2101

Hardy, J., and D.J. Selkoe. 2002. The amyloid hypothesis of Alzheimer's disease: progress and problems on the road to therapeutics. *Science.* 297:353–356. doi:10.1126/science.1072994

Herreman, A., L. Sermeels, W. Annaert, D. Collen, L. Schoonjans, and B. De Strooper. 2000. Total inactivation of gamma-secretase activity in presenilin-deficient embryonic stem cells. *Nat. Cell Biol.* 2:461–462. doi:10.1038/35017105

Hirsch, H.A., G.W. Jawdekar, K.A. Lee, L. Gu, and R.W. Henry. 2004. Distinct mechanisms for repression of RNA polymerase III transcription by the retinoblastoma tumor suppressor protein. *Mol. Cell. Biol.* 24:5989–5999. doi:10.1128/MCB.24.13.5989-5999.2004

Holmqvist, M.H., J. Cao, R. Hernandez-Pineda, M.D. Jacobson, K.I. Carroll, M.A. Sung, M. Betty, P. Ge, K.J. Gilbride, M.E. Brown, et al. 2002. Elimination of fast inactivation in Kv4 A-type potassium channels by an auxiliary subunit domain. *Proc. Natl. Acad. Sci. USA.* 99:1035–1040. doi:10.1073/pnas.022509299

Johnson, S.A., T. McNeill, B. Cordell, and C.E. Finch. 1990. Relation of neuronal APP-751/APP-695 mRNA ratio and neuritic plaque density in Alzheimer's disease. *Science.* 248:854–857. doi:10.1126/science.2111579

Kitagawa, H., W.J. Ray, H. Glantschnig, P.V. Nantermet, Y. Yu, C.T. Leu, S. Harada, S. Kato, and L.P. Freedman. 2007. A regulatory circuit mediating convergence between Nurr1 transcriptional regulation and Wnt signaling. *Mol. Cell. Biol.* 27:7486–7496. doi:10.1128/MCB.00409-07

McGeer, P.L., J. Rogers, and E.G. McGeer. 2006. Inflammation, anti-inflammatory agents and Alzheimer disease: the last 12 years. *J. Alzheimers Dis.* 9: 271–276.

Morohashi, Y., N. Hatano, S. Ohya, R. Takikawa, T. Watabiki, N. Takasugi, Y. Imaizumi, T. Tomita, and T. Iwatsubo. 2002. Molecular cloning and characterization of CALP/KCHIP4, a novel EF-hand protein interacting with presenilin 2 and voltage-gated potassium channel subunit Kv4. *J. Biol. Chem.* 277:14965–14975. doi:10.1074/jbc.M200897200

Pagano, A., M. Castelnuovo, F. Tortelli, R. Ferrari, G. Dieci, and R. Cancedda. 2007. New small nuclear RNA gene-like transcriptional units as sources of regulatory transcripts. *PLoS Genet.* 3:e1. doi:10.1371/journal.pgen.0030001

Parks, A.L., and D. Curtis. 2007. Presenilin diversifies its portfolio. *Trends Genet.* 23:140–150. doi:10.1016/j.tig.2007.01.008

Patel, S.P., D.L. Campbell, and H.C. Strauss. 2002. Elucidating KCHIP effects on Kv4.3 inactivation and recovery kinetics with a minimal KCHIP2 isoform. *J. Physiol.* 545:5–11. doi:10.1113/jphysiol.2002.031856

- Pruunsild, P., and T. Timmusk. 2005. Structure, alternative splicing, and expression of the human and mouse KCNIP gene family. *Genomics*. 86:581–593. doi:10.1016/j.ygeno.2005.07.001
- Rhodes, K.J., K.I. Carroll, M.A. Sung, L.C. Doliveira, M.M. Monaghan, S.L. Burke, B.W. Strassle, L. Buchwalder, M. Menegola, J. Cao, et al. 2004. KChIPs and Kv4 alpha subunits as integral components of A-type potassium channels in mammalian brain. *J. Neurosci.* 24:7903–7915. doi:10.1523/JNEUROSCI.0776-04.2004
- Schwenk, J., G. Zolles, N.G. Kandias, I. Neubauer, H. Kalbacher, M. Covarrubias, B. Fakler, and D. Bontrop. 2008. NMR analysis of KChIP4a reveals structural basis for control of surface expression of Kv4 channel complexes. *J. Biol. Chem.* 283:18937–18946. doi:10.1074/jbc.M800976200
- Selkoe, D.J. 1990. Deciphering Alzheimer's disease: the amyloid precursor protein yields new clues. *Science*. 248:1058–1060. doi:10.1126/science.2111582
- Shibata, R., H. Misonou, C.R. Campomanes, A.E. Anderson, L.A. Schrader, L.C. Doliveira, K.I. Carroll, J.D. Sweatt, K.J. Rhodes, and J.S. Trimmer. 2003. A fundamental role for KChIPs in determining the molecular properties and trafficking of Kv4.2 potassium channels. *J. Biol. Chem.* 278:36445–36454. doi:10.1074/jbc.M306142200
- St George-Hyslop, P.H., and A. Petit. 2005. Molecular biology and genetics of Alzheimer's disease. *C. R. Biol.* 328:119–130. doi:10.1016/j.crv.2004.10.013
- Trimmer, J.S., and K.J. Rhodes. 2004. Localization of voltage-gated ion channels in mammalian brain. *Annu. Rev. Physiol.* 66:477–519. doi:10.1146/annurev.physiol.66.032102.113328
- Wang, G., M.A. Balamotis, J.L. Stevens, Y. Yamaguchi, H. Handa, and A.J. Berk. 2005. Mediator requirement for both recruitment and postrecruitment steps in transcription initiation. *Mol. Cell.* 17:683–694. doi:10.1016/j.molcel.2005.02.010
- Waters, M.F., N.A. Minassian, G. Stevanin, K.P. Figueroa, J.P. Bannister, D. Nolte, A.F. Mock, V.G. Evidente, D.B. Fee, U. Müller, et al. 2006. Mutations in voltage-gated potassium channel KCNC3 cause degenerative and developmental central nervous system phenotypes. *Nat. Genet.* 38:447–451. doi:10.1038/ng1758
- Wu, L., J. Pan, V. Thoroddsen, D.R. Wysong, R.K. Blackman, C.E. Bulawa, A.E. Gould, T.D. Ocain, L.R. Dick, P. Errada, et al. 2003. Novel small-molecule inhibitors of RNA polymerase III. *Eukaryot. Cell.* 2:256–264. doi:10.1128/EC.2.2.256-264.2003
- Wyss-Coray, T. 2006. Inflammation in Alzheimer disease: driving force, bystander or beneficial response? *Nat. Med.* 12:1005–1015.